Slip Distribution of 15th January 1934 Bihar-Nepal earthquake (Mw 8.1)

[Keshav Kumar Sharma[1], Kumar Pallav[2], S. K. Duggal[3], Lav Joshi[4]]

Abstract—Slip distribution model has been developed for 15th January 1934 Bihar-Nepal earthquake of M_w 8.1 has been developed through stochastic model. The spatial variability of slip on the rupture plane is simulated as a random field with correlation lengths depending on the magnitude of the earthquake. The source dimensions have been computed from the scaling laws of Wells and Coppersmith (1994) and Mai and Beroza (2000). The slip distribution has been obtained from spectral synthesis method of Iguzquiza and Olma (1993) for both the source dimension. The slip distribution of each of the 5 samples has been shown in form of contour plots. The average slip estimated using different source dimension from WC and MB are 8.15 m and 12.96 m respectively. The simulated slip models developed can be used to simulate the displacement time histories of the 1934 Bihar-Nepal earthquake which can be used in seismic hazard studies in future

Keywords— Slip Distribution, Spectral Synthesis, Source Dimension, Bihar-Nepal Earthquake

I. Introduction

On 15th January 1934 at around 2:15 P.M. (I.S.T.) one of the most devastating earthquake occurred in the history of India and Nepal. Its epicentre was in a small village Tamku(27.55^oN 87.07^oE) in the Kosi Zone of north-eastern Nepal (Sapkota et al. 2013) having moment magnitude of M_w 8.1 (Ambraseys and Douglas, 2004). It caused widespread damage in Central and Eastern part of Nepal and in Northern India. The tremors from this earthquake were reported to be felt in Lhasa in China to Maharashtra in India and from Assam to Punjab covering an area of about 2,800,000 sq. km. The places in which there was evident damage to life and economy extended from Purnea in the east to Champaran in the west a distance of nearly 320 km and from Kathmandu in the north to Munger in the south a distance of nearly 130 km.

Keshav Kumar Sharma, Ph.D. Scholar,
Department of Civil Engineering,
MNNIT Allahabad-211004, India

Kumar Pallav, Assistant Professor,
Department of Civil Engineering,
MNNIT Allahabad-211004, India

S K. Duggal, Professor
Department of Civil Engineering,
MNNIT Allahabad-211004, India

Luv Joshi, Postgraduate Student,
Department of Civil Engineering,
MNNIT Allahabad-211004, India

The severity of the earthquake can be estimated from the fact that, in Kolkata which is more than 600 km from the epicentre many buildings were damaged and the tower of St. Paul's Cathedral collapsed.(Nobuji N. 1934).The observed damage was most severe in two parallel belts in the plains of India and in the Kathmandu valley. The zones of highest intensity were not found to be concentric; the most peculiar fact about the intensity and the inferred damage distribution was the existence of numerous cases of rapid and incomprehensible changes in intensity throughout the area (Dunn et al. 1939). The location of the study region has been shown in Figure 1a

Objective And Scope Of Work

Four major earthquakes of moment magnitude greater than 8 have occurred in the Himalayan foothills in last 125 years namely 1897 Assam earthquake, 1905 Kangra earthquake, 1934 Bihar-Nepal earthquake and 1950 Assam earthquake. They have caused widespread damage and resulted in loss of thousands of lives. It is a well-known fact that there is an accelerated growth in the population density as well as in the infrastructural development in the affected areas which directly implies that the vulnerability of the region has increased immensely in last 125 years (Arya, 1990). Thus the occurrence of a similar episode in the present day scenario will be disastrous. The most likely sites for the next events are the seismic gaps between the 1905 Kangra and 1934 Bihar-Nepal earthquakes and between the Kangra earthquakes and the Taxila, Pakistan, earthquake of AD 25 (Yeats et al 1998). As a result, it is necessary to work out a dependable estimation of seismic hazard in this region. The major sub-surface faults in this region have been shown in Table 1 and the seismotectonic map of the study region has been shown in Figure 1(b). Solely speaking from the engineering point of view the most important information from an earthquake is the peak ground acceleration and response spectra. Strong motion accelerograms (S.M.A.) are used to obtain these parameters, but S.M.A. records are not available for the 1934 event. Hence, the ground motion parameter for this event has to be obtained using seismological models in which the source path and site effects are specified analytically. The aim of the present study is to know the slip distribution models that describe the amount and distribution of slip associated with the 1934 event, which can be used to predict any strong ground motion in future. The estimation of the simulated ground motion parameters will contribute in acquiring critical information on the related seismic hazard, which will aid in establishing better earthquake resistant design codes.
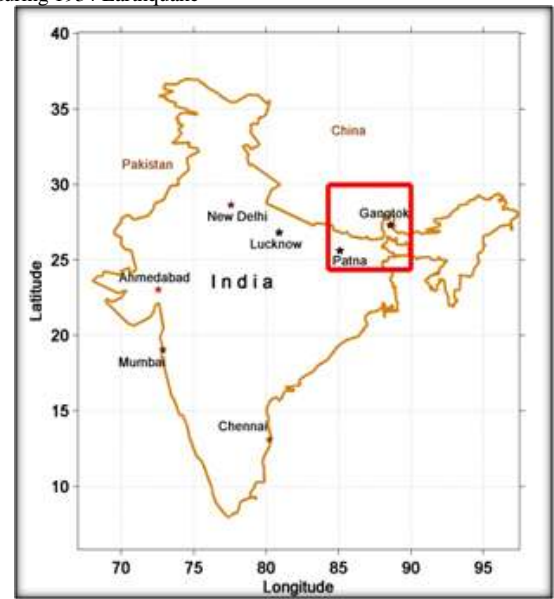
II Damage and Economic Losses

Major damage in India was reported in four cities along the Ganga river between Monghyr and Patna, of which Monghyr was the worst effected town in Bihar. The entire town was reduced to ruins, scarcely a house or hut escaped
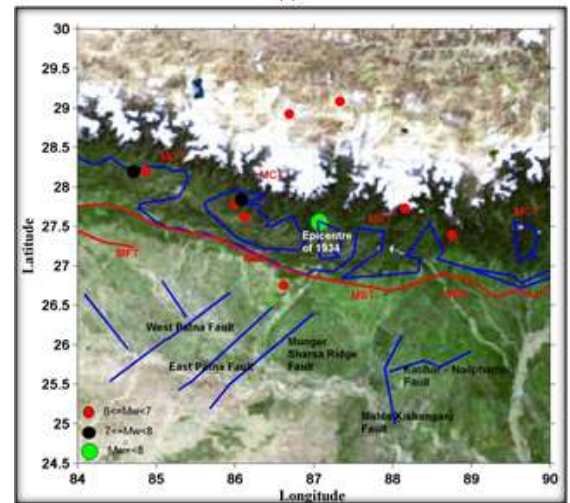
damage or destruction (Dunn et al. 1939). Buildings on rock projections received less damage than those on alluvium. The root cause of damage to buildings in Monghyr was shaking, neither fissures nor was slumping of the ground apparent apart from near the bank of the river in the north. Similarly in Patna and Barh the effect of the earthquake was notable only towards the bank of river Ganges. The damages reported in India and lack of any particular orientation of the fissures and the abundance of sand and water in the fissures advocate that this disruption of the earth's surface was limited to superficial layers and not to faulting of the basement beneath that area. The damage and destruction in Nepal was mostly around Kathmandu valley. Few causalities were reported and few houses were damaged to the west of Kathmandu than east of it. One of the majorly affected towns, where the damage was quite pronounced, was Bhaktapur and its neighboring villages in the eastern part of the valley. In the areas west and north of the Kathmandu valley the damage was found to be most severe in Syabru (Figure 1(c)). In other towns namely Nawakot, Trisuli, Bazar and Betrawati damage was confined to large and small cracks. Following the report from Rana et al.(1935) the temple of Nawakot Bhairabnath was fractured all around and the upper floors were tilted. The northern portion of the guesthouse of the temple of Sri Bharaibi was destroyed; the roof settled on both sides. In Gurkha the upper palace with the Temple of Sri Kalika Devi was damaged. In Kaski instances of landslides were reported. In the areas east of Kathmandu, nearly half of the people scummed to death and most of the houses got destroyed from the mountainous area east of Kathmandu in all the districts up to the border. In Tibet, all government buildings were destroyed including storehouses and barracks. The damage from the eastern border of Nepal to Chitwan was quite apparent, both destruction and loss of life were more in towns than in smaller villages. It was because in the latter houses were built of bamboo and covered with thatched roofs. There were fissures essentially everywhere, reported by Rana et al. (1935) as wide as 3 to 4 meters and as deep as 20 to 30 meters. The total causalities reported by Rana et al.(1935) was 8519 in Nepal and about 7253 in Bihar (Brett W.B. 1935).

Table1 Major sub-surface faults and their length in the epicentre region

Sl. No.	Name of the Fault	Length (km)
1.	West Patna Fault	212.26
2.	East Patna Fault	174.59
3.	MungerSharsa Ridge Fault	219.05
4.	MungerSharsa Ridge Marginal	154.44
5.	MaldaKishanganj Fault	133.50
6.	KatiharNailphami Fault	114.28

III Past Studies

In past many studies were performed on the slip distribution of earthquakes. The seismic slip distribution along the San Jacinto Fault Zone, Southern California has been analysed by Thatcher et al. (1975). Freymuellar et al. (1994) discussed the co-seismic slip distribution of the Landers Earthquake using a model on the inversion of surface geodetic measurements; primarily the vector

displacements were measured using the Global Positioning System (GPS).
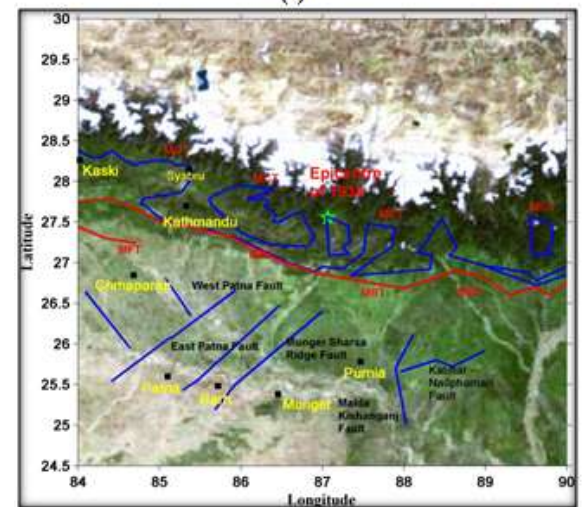
Figure 1. (a) Location of study region (Lat 24^0N -30^0N, Long 84^0E- 90^0E) (b) Seismotectonic setup near epicenter (GSI, 2000)   (c) Major cities affected during 1934 Earthquake

(a)

(b)

(c)

Slip distribution of the 2003 Boumerdes-Zemmouri earthquake, Algeria, from teleseismic, GPS and coastal

2

uplift data has been developed by Delouis B. et al. (2004).. The fault slip distribution for the Chi –Chi Taiwan earthquake has been determined by Zhang et al. (2010) with the observed GPS coseismal displacements as well as interferometric synthetic aperture radar (InSAR) data. Slip distribution of the 1952 Kamchatka earthquake based on near-field tsunami deposits and historical records has been developed by Breanyn et al. (2010). Romano F. et al. (2014) established the structural control on the Tohoku earthquake rupture process using 3D FEM, tsunami and geodetic data. Singh and Gupta(1980) determined the source mechanism of the 1934 Bihar-Nepal earthquake using the P-wave first motions, S-wave polarization angles, and surface-wave spectral data.In present scenario, due to availability of advance techniques, slip distribution can be analysed precisely.Wilkinson et al. (2014) used LiDAR and field mapping of geomorphic offsets to analyse the slip distributions on active normal faults.

IV Methodology

The fault plane solutions reveal the geometry and mechanism of the fault are developed using the teleseismic data which contributes towards a preliminary impression about the source. However it is not sufficient to compute ground motion which is used in engineering problems. The motion near the source is predominantly influenced by the spatial and temporal variability of the fault slip. Due to the unavailability of the finite-fault slip model for the 1934 event the slip distribution needs to be defined by some other method. In such cases stochastic models are more useful to enumerate the slip distribution on the rupture plane. In the present study spatial variability of slip on the rupture plane is simulated as a random field and is plotted as contour using MATLAB software. The slip distribution along the fault surface is calculated using the spectral synthesis method, Iguzquiza P.E. et al (1993), in which the slip-amplitude spectrum is defined through a spatial auto-correlation function, and the entire field obeys Hermitian symmetry. For the computation of source dimensions the details of surface rupture length (if surface rupture occurred) or the spatial extent of early aftershocks is required. Due to absence of these data sets for the 1934 event, the scaling laws of Mai and Beroza(2000) and Wells and Coppersmith (1994) are used for the calculation of source dimensions. Both of these methods are disused as follows.

Wells and Coppersmith (1994)

Wells and Coppersmith compiled the source parameters of various historical earthquakes and on the basis of regression analysis they developed empirical relationships among moment magnitude, rupture length, and down-dip rupture width which is given in Eq 1.0,

$$log (RL) = a + b*M \qquad (1)$$

where, RL is the rupture length, a and b are coefficients, and M is the moment magnitude of the earthquake

Wells and Coppersmith (1994) performed regression analysis of 43 events with strike slip mechanism. The values for the coefficients a and$b$ were found to be -3.55 and 0.74, respectively and with standard errors of 0.37 and 0.05, respectively. The standard deviation was found to be 0.23, the correlation coefficient was 0.91 and this equation was validated for a range of magnitude of 5.6 to 8.1.

$$log(RW) = a + b*M \qquad (2)$$

where, RW is the down-dip rupture width, a and b are coefficients, and M is the moment magnitude of the earthquake.

Table 2 List of Parameters

S. No.	Parameter	Value	
1.	Magnitude	8.1	
2.	Mechanism	Strike-Slip	
3.	Auto-Correlation Function	Von Karman	
4.	Correlation Length	Along Strike	70.6318 km
		Dip Direction	11.2980 km
5.	Hurst Exponent	0.7749	
6.	Maximum Depth	15km	
7.	Dip Angle	45°	

After the regression analysis of 87 events with strike slip mechanism the values for the coefficients a and b were found to be -0.76 and 0.27, respectively and with standard errors of 0.12 and 0.02, respectively. The standard deviation was found to be 0.14, the correlation coefficient was 0.84 and this equation was validated for a range of magnitude of 4.8 to 8.1.

Mai and Beroza(2000)

For the analysis of slip heterogeneity Mai and Beroza(2000) calculated source dimensions based on the autocorrelation width. For a given function f, let the autocorrelation width beW_{ACF}, is the area under the autocorrelation function of that function as given in Eq. 3.0

$$(3)$$

Using this formulation the calculation of effective length and effective width of the fault from one dimensional slip function is done. The one dimensional slip function is computed by summing the slip values in the individual sub-faults in down-dip and along strike direction.

The magnitude of the earthquake is taken to be 8.1 (Ambraseys and Douglas (2004)) and the faulting mechanism is assumed to be strike-slip. From the study of Mai and Beroza (2002) in which they modeled slip distribution of numerous former earthquakes, it is concluded that the best fit of the data was obtained by Von Karman distribution in which the Hurst exponent to be considered is approximately 0.75. The correlation lengths are calculated from the scaling relations of Mai and Beroza (2002) which is as follows

$$log(a)=b_0 + b_1 M_w \qquad (4)$$

where a is the Von Karman Correlation Length , b_0 is the slope error, b_1 is the intercept error, and M_w is moment magnitude of the earthquake. The value of b_0 and b_1 along strike direction is given as 0.59 and -2.93, respectively and for down dip direction, it is given as 0.33 and-1.62, respectively for strike slip mechanism. Using these values the correlation length along strike is calculated to be70.6318 km and in the dip direction it is 11.2980 km ; Hurst exponent is adopted to be 0.7749. Apart from these calculated values, the maximum depth of the fault is assumed to be 5 km for the Himalayan region and the dip angle of fault plane is taken as 45°.

All these parameters have been summarised in Table 2. Knowing these values the slip discrepancy is described by the Von Karman power spectral density function as

$$(5)$$

where a_x is the correlation length along the strike, a_z is the correlation length along the dip, k is the wave number and H is the Hurst exponent.

Further, while plotting the contours the non-linear scaling exponent for the random field is taken to be 1.3 to roughen the field, which flattens the spectrum. This helps in simulation of slip distribution with large peak-slip values.

V   Results and Discussion

The plots that show the distribution of slip along the direction of strike and in the down-dip direction have been shown in the form of contours. Five samples each have been plotted using the source dimensions of Mai and Beroza (2000) Figure 2 and Wells and Coppersmith (1994) Figure 5. Figure 3(a) shows the variation of slip along the direction of strike for a fixed value of strike of 100km, obtained using the source dimensions of Mai and Beroza (2000). The value of 100km is specifically chosen as this is the point along which maximum variation is noticed in the plotted contours, by visual inspection. From the figure it can be very clearly inferred that the distribution is somewhat similar in all the five cases, and an alternating rising and falling trend is observed in the values of slip. Figure 4(a) shows the variation of slip in the down-dip direction for a fixed value of dip of 10 km, obtained using the source dimensions of Mai and Beroza (2000). The value of 10 km is specifically chosen as this is the point along which maximum variation is noticed in the plotted contours, by visual inspection. From the figure it can be clearly inferred that the distribution is somewhat similar in all the five cases, and no sudden change in gradient or discontinuity etc. is observed. From Figure 7(a) which shows the same variation for the same value of dip of 10km using the source dimension of Wells and Coppersmith (1994) it is seen that the variations are comparatively more discrete, but the range of the variation is lower with the highest values of slip being in the range of 2000cm to 2500 cm, where as it is in the range of 3000cm in the former case. A comparative observation of variation of average values of slip obtained from both the methods for the same point, dip of 10km has been shown. Figure 4(b) and Figure 7(b) which contains both the plots obtained shows that the method of Mai and Beroza (2000) yields a more symmetrical trajectory as compared to that obtained from Wells and Coppersmith (1994) source dimensions showing a rising trajectory.

Table 3 Average Slip

S. No.	Average Slip from Mai and Beroza(2000)	Average Slip from Wells and Coppersmith(1994)
Sample 1	12.848 m	9.251 m
Sample 2	11.974 m	8.864 m
Sample 3	14.554 m	8.052 m
Sample 4	12.101 m	6.146 m
Sample 5	13.348 m	8.439 m
Average of 5 Samples	12.965 m	8.1504 m

From Figure 6(a) which shows the same variation for the same value of strike of 100km using the source dimension of Wells and Coppersmith (1994), it is seen that the variations

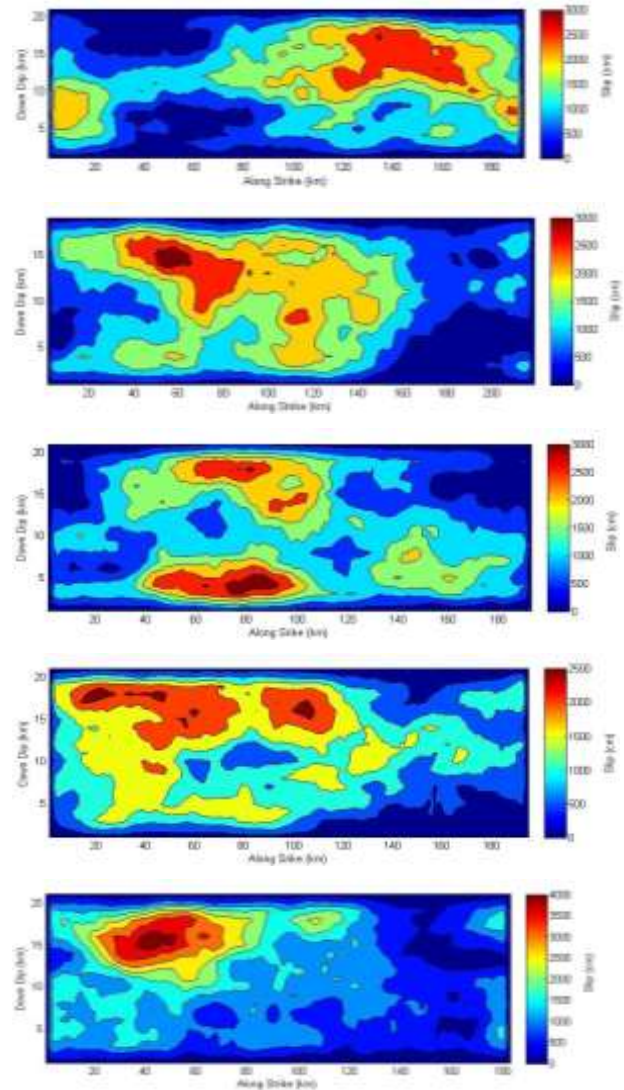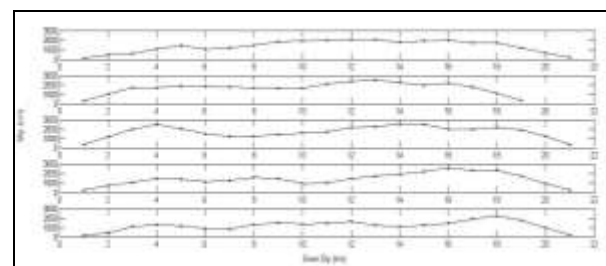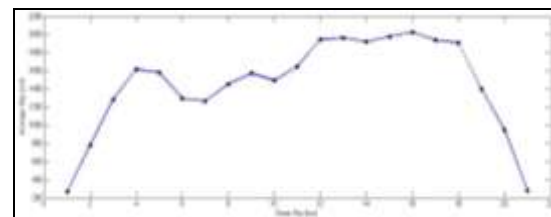here follow a flatter distribution without the presence of any sharp peak or drop.

Figure 2 *Sample slip field on rupture plane for 1934 Bihar-Nepal earthquake, Mw 8.1 (Mai and Beroza, 2000)*

(a)

(b)

Figure 3. Variation of displacement at strike of 100 km along the fault (a) Five samples obtained from the source dimension (Mai and Beroza, 2000) (b) Average of five samples
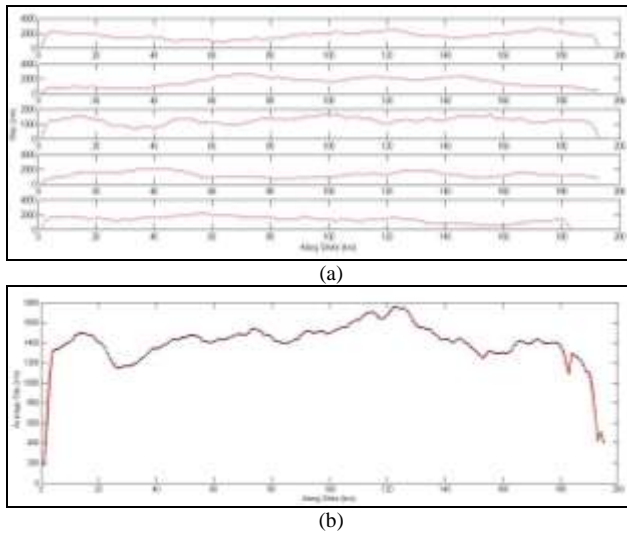
4

(a)

(b)

Figure 4 Variation of displacement at dip of 10 km along the fault (a) Five samples obtained from the source dimension (Mai and Beroza, 2000), (b) Average of five samples
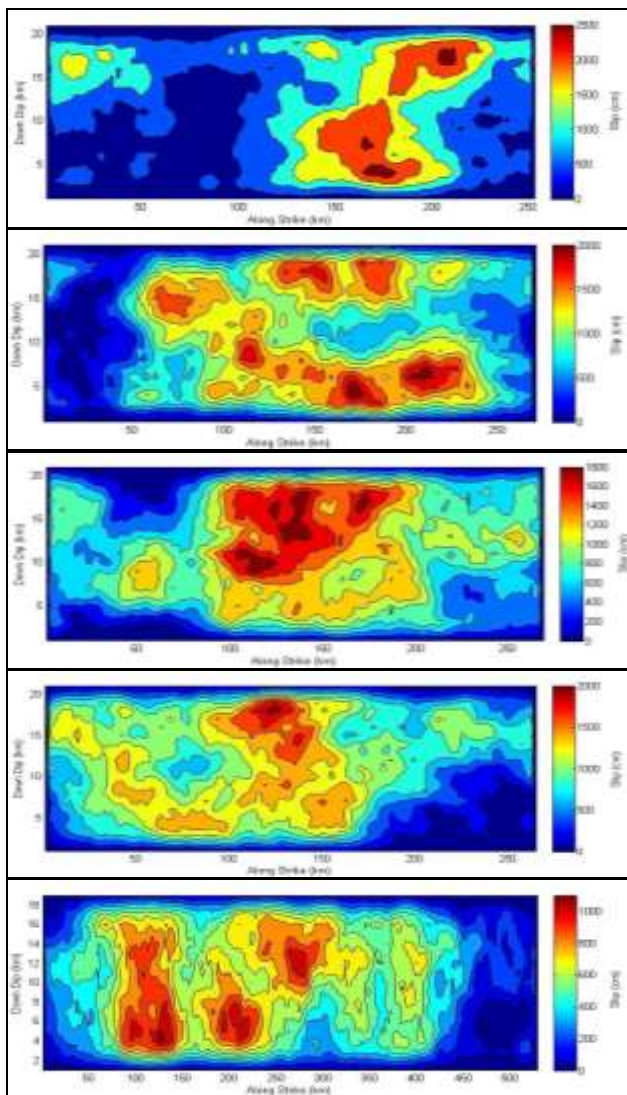

Figure 5. Sample slip field on rupture plane (Wells and Coppersmith, 1994)

A comparative observation has also been shown for variation of average values of slip obtained from both the methods for the same point, and for strike of 100km. Figure 3(b) and Figure 6(b) contain both the plots obtained,

showing that both the methods have somewhat similar trends, with an initial rising phase followed by an intermediate flat phase and finally a gradually dropping phase. The average slip obtained from each sample is given in Table 3. From the comparison of average slips in the cases, it is evident that the value of slip obtained using the scaling laws of Wells and Coppersmith (1994) which is 8.1504 m is lower than that obtained from Mai and Beroza (2000) which is 12.965 m. The final results obtained are in agreement with the trends noticed by Wells and Coppersmith (1994).
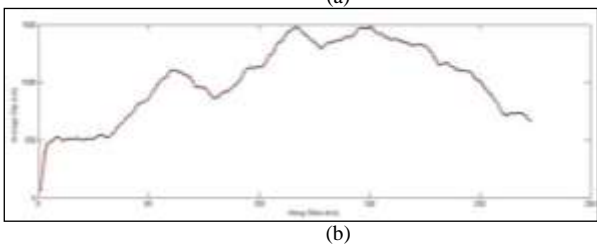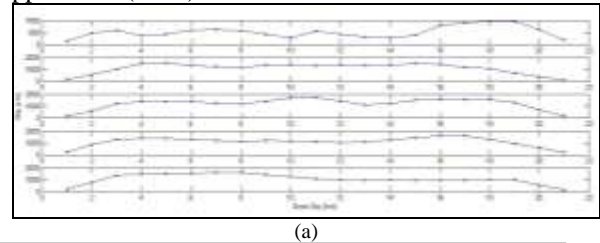

(a)

(b)

Figure 6. Variation of displacement at strike of 100 km along the fault (a) Five samples obtained from the source dimension (Wells and Coppersmith, 1994), (b) Average of five samples
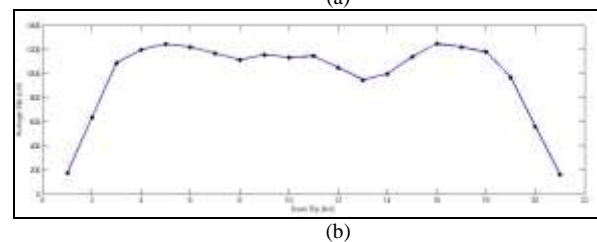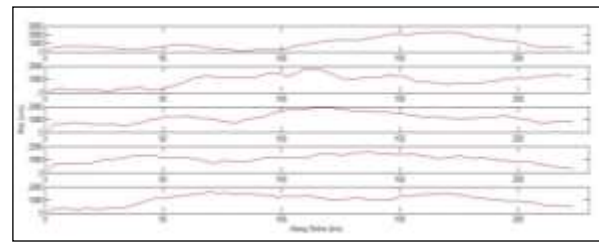

(a)

(b)

Figure 7. Variation of displacement at dip of 10 km along the fault (a) Five samples obtained fromthe source dimension (Wells and Coppersmith,1994), (b) Average of five samples

VI Conclusions

Of all the factors that influence the seismic risk of a particular region, vulnerability is the one which can be controlled by the engineers. The evident increase in population and more importantly the faulty construction practices, which are presently not up to mark, are the main causes in the escalation of the vulnerability in central and eastern part of Nepal and in Northern India. The present study will help in the development of displacement time histories which will be of varied use in the infrastructural

development in central and eastern parts of Nepal and in Northern India. The developed ground motions can be used as an aid to figure out the probable damage that could occur in this region due to a similar earthquake, so that preventive measures can be taken to avoid a great loss of life and property in the future

References

[1] Sapkota, S. N., Bollinger, L., Klinger, Y., Tapponnier, P., Gaudemer,Y. and Tiwari, D., Primary surface ruptures of the great Himalayan earthquakes in 1934 and 1255. Nature Geosci., 2013, pp.71–76

[2] NobujiNasu, The Great Indian Earthquake of 1934, Earthquake Research Institute,1934

[3] Dunn, J. A., Auden, J. B., Ghosh, A. M. and Wadia, D. N., The Bihar–Nepal Earthquake of 1934. Geol. Surv. India Mem., 1939,73, 205.

[4] U.S.G.S. (United States Geological Survey) http://www.usgs.gov, retrieved on 15th May,2015.

[5] Seismotectonic Atlas of India and its Environs, Geological Survey of India.

[6] Arya A.S., Bull. Indian Soc. Earthquake Tech, 1990 27,12

[7] Yeats S. R., and Thakur C. V., Reassessment of earthquake hazard based on a fault-bend fold model of the Himalayan plate-boundary fault. Current Science, 1998, 74

[8] Rana, Maj. Gen. Braham Sumsher J.B., NepalkoBhukampaThe Great Earthquake of Nepal,1935.

[9] A report on the Bihar Earthquake and on the measures taken in consequence thereof up to 31 December 1934. W.B. Brett, Relief Commissioner, Bihar and Orissa. Superintendent, Government Printing, Bihar and Orissa, Patna, 1935.

[10] Zhang L.,WuC.J.,GeL.L.,Ding X.L., and Chen Y.L., Determining fault slip distribution of the Chi-Chi Taiwan earthquake with GPS and InSAR data using triangular dislocation elements. Journal of Geodynamics,2008

[11] Romano F., Trasatti E., Lorito S., Piromallo C., Piatanesi A., Ito Y., Structural control on the Tohoku earthquake rupture process investigated by 3D FEM, tsunami and geodetic data. Scientific Reports,2014.

[12] Singh D.D., and Gupta K.H., Source dynamics of two great earthquakes of the Indian subcontinent: The Bihar-Nepal earthquake of January 15,1934 and the Quetta earthquake of May 30,1935. Bulletin of the Seismological Society of Amrecia, Vol 70,No. 3, June 1980.

[13] FreymuellerJ.,King N.E., and SegallP.,The Co-Seismic Slip Distribution of the Landers Earthquake, Bulletin of the Seismological Society of America, 1994; Vol. 84, No. 3, pp. 646-659.

[14] Breanyn T. MacInnes, Robert Weiss, Joanne Bourgeois, and Tatiana K. Pinegina, Slip Distribution of the 1952 Kamchatka Great Earthquake Based on Near-Field Tsunami Deposits and Historical Records. Bulletin of the Seismological Society of America, Vol. 100, No. 4, pp. 1695–1709, August 2010.

[15] Delouis B., Valle´e M., MeghraouiM.,Calais E.,Maouche S., Lammali K., Mahsas A.,Briole P.,Benhamouda F., and Yelles K.. Slip distribution of the 2003 Boumerdes-Zemmouri earthquake, Algeria, from teleseismic, GPS, and coastal uplift data. Geophysical research letters, 31,2004.

[16] Kurt L. Feigl, Francesco Sarti, He´le`neVadon, Simon McClusky, SemihErgintav, Philippe Durand, Roland Bu¨rgmann, Alexis Rigo, Didier Massonnet, and Rob Reilinger.Estimating Slip Distribution for the I˙zmitMainshock from Coseismic GPS, ERS-1, RADARSAT, and SPOT Measurements, Bulletin of the Seismological Society of America, 92, 2002.

[17] Wilkinson, M. and Roberts, Gerald P. and McCaffrey, K. and Cowie, P.A. and Faure Walker, J.P. and Papanikolaou, I.D. and Phillips, R.J. and Michetti, A.M. and Vittori, E. and Gregory, L. and Wedmore, L. and Watson, Z, Slip distributions on active normal faults measured from LiDAR and field mapping of geomorphic offsets: an example from L'Aquila, Italy, and implications for modelling seismic moment release, Science Direct,2014

[18] Thatcher W., Hileman A.J., and Hanks C.T., Seismic Slip Distribution along the San Jacinto Fault Zone, Southern California, and Its Implications, Geological Society of America Bulletin,1975

[19] Das, S., and C. Henry, Spatial relation between main earthquake slip and its aftershock distribution, Rev. Geophys., 41(3), 1013, 2003.

[20] Pardo-Igúzquiza E. and Chica-Olmo M., The Fourier Integral Method: An efficient spectral method for simulation of random fields, Mathematical Geology, 25,1993.

[21] Mai, P.M., and G.C. Beroza. A spatial random-field model to characterize complexity in earthquake slip, J. Geoph. Res., 107(B11), 2308, doi:10.1029/2001JB000588, 2002.

[22] Mai, P.M., and G.C. Beroza. Source-scaling properties from finite-fault rupture models, Bull. Seis. Soc. Am., 90,604-615, 2000.

[23] Wells, D. L., and K. J. Coppersmith. New empirical relationships among magnitude, rupture length, rupture width, rupture area, and surface displacement, Bull. Seism. Soc. Am. 84, 974–1002,1994.

[24] Molnar, P. and Deng, Q., Faulting associated with large earthquakesand the average rate of deformation in central and easternIndia. J. Geophys. Res., 1984, 89, 6203–6227

[25] Bilham, R., Blume, F., Bendick, R. and Gaur, V. K., Geodeticconstraints on the translation and deformation of India: implicationsfor future great Himalayan earthquakes. Curr. Sci., 1998, 74,213–229